| Sl. No.	**IIT Ropar** **List of Recent Publications with Abstract** **Coverage: April, 2021**
1.	A comprehensive analysis of the trip frequency behavior in COVID scenario Bh Aaditya, TM Rahul - Transportation Letters, 2021 **Abstract:** The fear of infection of COVID-19 among people has greatly reduced their intention to travel, which needs a deeper understanding to aid the policy-makers in framing robust guidelines to ensure safe travel. This paper aims to present a critical understanding of the traveler's willingness to reduce their trip frequency, using psycho attitudinal analysis of the variables impacting the travel behavior. For this purpose, a web-based survey was conducted across India, and demographic, socio economic and psycho-attitudinal data was collected from 410 individuals, from across 21 states of India. Information regarding the psycho-attitudinal data was collected using a set of indicators. After extraction of latent factors from these indicators using factor analysis, factor scores were determined for each individual for these latent factors. Subsequently, ordered logistic regression models were used to understand the influence of these pandemic-oriented variables upon an individual's intention to travel for essential, recreational and work trips. In the estimation results, majority of the respondents showed a willingness to reduce their essential and recreational trips compared with work trips. The awareness regarding the disease and the regionality of respondents showed a significant influence on their decision. The study concludes by presenting the policy implications of the analysis.
2.	A Parallel Cyclic Reduction Algorithm for Pentadiagonal Systems with Application to a Convection-Dominated Heston PDE A Ghosh, C Mishra - SIAM Journal on Scientific Computing, 2021 **Abstract:** Based on the parallel cyclic reduction technique, a promising new parallel algorithm is designed for pentadiagonal systems. Subject to fulfilling stability conditions, this highly parallelizable algorithm works very well for systems of any size. The solver is implemented on a graphics processing unit using the CUDA programming platform where it is empirically studied for its performance in comparison with some of the present-day prominent parallel solvers. The construction of the new algorithm is originally motivated by a real-world application in computational finance. Accordingly, it is employed successfully to numerically solve the convection-dominated Heston partial differential equation for pricing a financial option, and implementation of the full solver is discussed in detail.
3.	An Analytical Frame Work to Design Planar Transmitting Array Antennas to Mitigate Lateral Misalignment in the Wireless Power Transfer Systems A Sharma, A Bharadwaj, VK Srivastava - IEEE Transactions on Antennas and Propagation, 2021 **Abstract:** This paper presents a unique mathematical analysis of the magnetic field (H-field) forming using coil antennas to mitigate the lateral misalignment problem in the wireless power transfer (WPT) system. State of the art emphasizes generating uniform H-field distribution as a solution to the stated problem and for that large-sized transmitters are designed to enhance receiver working region. In this paper, by optimizing the field forming technique based on derived closed-form analytical expressions, a general non-uniform H-field distribution is proposed as an optimal solution to the misalignment problem. Through rigorous analysis, this

	work proposes a step-wise procedure for designing the transmitter coil array antenna to generate the non-uniform H-field distribution. To validate the model, two planar antenna arrays are designed by following the proposed procedure. This results in a uniform induced voltage profile under the misaligned Rx condition, hence, resolves the problem. The antenna designs are simulated, fabricated, and measured. The analytical results are found in agreement with the simulated results and further verified experimentally. The results indicate that the antennas designed using the proposed method are able to mitigate the lateral misalignment problem in a wider area of the receiver region with a smaller transmitter size.
4.	An approach to early stage detection of atherosclerosis using arterial blood pressure measurements K Jain, S Jain, A Guha, A Patra - Biomedical Signal Processing and Control, 2021 **Abstract:** Atherosclerosis is a pathological condition that develops gradually over the years and may eventually lead to a heart attack, a stroke, or a peripheral vascular disease, depending upon its site of occurrence in the human arterial network. We aim to detect this pathological condition in its early stage so that the necessary measures can be taken timely. To achieve this, a third-order nonlinear model of the cardiovascular system is considered, having states as systemic arterial and venous pressures along with the left ventricular volume. The available measurement signal is arterial blood pressure taken from the radial artery. This paper proposes the idea of online tracking of model parameters by utilizing an unscented Kalman filter (UKF) based framework that would help monitor the above-mentioned pathological condition. Furthermore, a classification approach has been presented, which carries out screening of subjects suffering from atherosclerotic cardiovascular diseases (CVDs) while utilizing estimates obtained from the UKF framework. It is observed that clinical quantities such as arterial compliance, systolic blood pressure, and ventricular elastance play an important role in the development of atherosclerosis. The classification results are quite encouraging. The proposed framework regularly monitors the atherosclerotic condition and has a potential for the early-stage screening of subjects suffering from atherosclerosis. With an increase in sedentary lifestyle in modern world, an early-stage screening of atherosclerotic cardiovascular diseases would be an important contribution to the healthcare and biomedical community.
5.	An Interaction Less Duo Control Strategy for Bi-polar Voltage Source Converter in Renewables Integrated Multi-Terminal HVDC (MTDC) Grids AS Kumar, BP Padhy - IEEE International Conference on Power Electronics, Drives and Energy Systems, 2020 **Abstract:** The PVF or PV^2F double droop control is commended for its ability to regulate both the dc voltage and frequency in a decentralized approach. However, a convincing response is not achieved due to an interaction between the droop characteristics of dc voltage and frequency. This interaction affects the dc voltage and frequency support of the AC system surrounded the Multi-Terminal HVDC (AC-MTDC) grid. To overcome this effect a interaction less Duo control strategy is proposed in this paper, which takes the advantage of a Bi-polar Voltage Source Converter (B-VSC) topology in the MTDC grid. The virtue of the proposed control technique is emphasized by comparing it with the existing PV 2 F double droop control along with two case studies. The validation of interaction less Duo control strategy is carried out on five terminal CIGRE DC grid benchmark model integrated into two area power system, which is simulated in PSCAD/EMTDC software.

6.	[Buoyancy effects in vertical 2-D and 3-D T-channels on the onset of flow reversal of power-law fluids in the side branch](#) A Maurya, N Tiwari, RP Chhabra - International Journal of Heat and Mass Transfer, 2021 **Abstract:** The primary goal of the present study is to investigate the flow reversal in the side branch of a T-channel for the flow of power-law fluids. The governing equations have been solved over wide ranges of conditions as: channel Reynolds number, $20 \leq Re \leq 100$, Prandtl number, $1 \leq Pr \leq 100$, Richardson number, $0 \leq Ri \leq 10$, power-law index, $0.2 \leq n \leq 1.4$, together with the conditions of equal exit pressure (EEP) and specified flow split (SFS). The flow reversal occurs in the side branch of the T-channel at a critical value of the Richardson number for the equal exit pressure condition, and this can be eliminated by using the specified flow rates as $10 \leq \beta MB (\%) \leq 99$ where, βMB is the value of the specific flow rate at the main branch outlet for a particular case. The results are interpreted in terms of velocity and temperature fields, exit flow rates, the required pressure to maintain the specific flow rate, recirculation lengths and the local Nusselt number. As the power-law index and/or Reynolds number is increased, the flow reversal is encountered at lower Richardson and Prandtl numbers. The flow rate from the main branch increases with Re, n, Ri while it decreases with Pr. Furthermore, the required pressure to maintain the flow rate shows a positive dependence on n, Ri and Pr whereas it shows an inverse dependence on Re and specified flow rates (βMB). Also, the rate of heat transfer rises with an increase in Re, Ri, Pr and β while it is promoted in shear-thinning fluids and impeded in shear-thickening fluids. Furthermore, the present work also compares the critical value of Richardson number of the 2-D model with that of the 3-D model for aspect ratio as $0.5 \leq AR \leq 10$. The results show that for $AR \geq 5$, the three-dimensional effects are small. Qualitative trends of the critical Richardson number e.g., with respect to Prandtl number obtained from the 3-D model are the same as from the 2-D model irrespective of the values of the aspect ratio.
7.	[Common Mode Impedance Shaping Choke to Attenuate the Conducted EMI in Three Phase Drive](#) M Kumar, K Jayaraman - IEEE International Conference on Power Electronics, Drives and Energy Systems, 2020 **Abstract:** This paper presents an impedance shaping technique to reshape the common mode (CM) impedance profile of three phase common mode choke. The CM impedance offered by a designed CM choke with specific core area and number of turns is reshaped using CMIS choke. CM noise in a two level voltage source inverter (TL-VSI) has dominant frequency components near inverter switching frequency (Fsw). Attenuation of these dominant frequency components demand high impedance at Fsw . A designed CMIS choke offers high CM impedance for Fsw compared to CCM choke. The proposed three phase CMIS choke is a passive CM noise attenuation technique that attenuates the dominant Fsw components. The CM attenuation performance of passive EMI filter with CMIS choke and CCM choke are compared for TL-VSI.
8.	[Comparative performance of magnetorheological external finishing tools using different magnetic structures](#) TS Bedi, R Kant - Materials Today: Proceedings, 2021 **Abstract:** The operative functionality of various mechanical parts depends on surface characteristics; therefore, surface roughness becomes vital for reducing the friction between the two mating surfaces. Currently, the grinding operation is used for finishing these mechanical

	parts. The grinding tool is generally made by the bonded abrasive particles that contact the part surface during the finishing operation. In grinding, the finishing forces induced by the grinding tool are uncontrollable, which makes the process less effective for nano-finishing applications. Magnetorheological (MR) finishing technique is considered as a better option for nano-finishing applications. In this work, MR finishing tools with flat and curved cylindrical magnets are developed, which has the advantage of being flexible according to the diameter of cylindrical parts. Magnetostatic simulations are carried out to visualize the distribution of magnetic flux density using the developed tools. The experimentation was performed using the developed tools with parameters: workpiece rotation of 440 rpm, linear tool feed of 10 cm/min and tool travel path along x-axis of 3 cm during finishing of the external cylindrical surface of a stainless-steel workpiece. Results showed that after 60 min of finishing, the surface roughness (R_a) was decreased by 62.74% for curved cylindrical magnets and 53.81% for flat cylindrical magnets.
9.	[Density Functional Theory Study of Li-Functionalized Nanoporous R-Graphyne–Metal–Organic Frameworks for Reversible Hydrogen Storage](#) RY Sathe, M Ussama, H Bae, H Lee, TJ Dhilip Kumar - ACS Applied Nano Materials, 2021 **Abstract:** Hydrogen is the most convenient recourse to shift from fossil fuels to an efficient and sustainable source of energy in automobiles. Achieving a high hydrogen weight percentage while storing hydrogen is the prime challenge in using hydrogen fuel. In the current study, a nanoporous metal–organic framework of 2.069 nm pore size having R-graphyne as a linker (G^R–MOF) is reported for the first time. Employing density functional theory, the hydrogen sorption characteristics of G^R–MOF functionalized with Li and its mechanism are investigated. A Kubas-like mechanism is observed in the process of hydrogen adsorption with sorption energies in the 0.25–0.27 eV range, with the highest hydrogen weight percentage of 11.95%. It is observed during the van 't Hoff desorption and Born–Oppenheimer molecular dynamics study that G^R–MOF reversibly stores hydrogen under operable thermodynamic conditions (100–300 K, 1–3 atm). G^R–MOF stands out to be a prospective material for reversible hydrogen storage under the norms set by the Department of Energy, USA.
10.	[Distinct Modes of Tissue Expansion in Free Versus Earlier-Confined Boundaries for More Physiological Modeling of Wound Healing, Cancer Metastasis, and Tissue Formation](#) A Kiran, N Kumar, V Mehandia - ACS Omega, 2021 **Abstract:** Collective cell migration is often seen in many biological processes like embryogenesis, cancer metastasis, and wound healing. Despite extensive experimental and theoretical research, the unified mechanism responsible for collective cell migration is not well known. Most of the studies have investigated artificial model wound to study the collective cell migration in an epithelial monolayer. These artificial model wounds possess a high cell number density compared to the physiological scenarios like wound healing (cell damage due to applied cut) and cancer metastasis (smaller cell clusters). Therefore, both systems may not completely relate to each other, and further investigation is needed to understand the collective cell migration in physiological scenarios. In an effort to fill this existing knowledge gap, we investigated the freely expanding monolayer that closely represented the physiological scenarios and compared it with the artificially created model wound. In the present work, we report the effect of initial boundary conditions (free and confined) on the collective cell migration of the epithelial cell monolayer. The expansion and migration aspects of the freely expanding and earlier-confined monolayer were investigated at the tissue and cellular levels. The freely

expanding monolayer showed significantly higher expansion and lower migration in comparison to the earlier-confined monolayer. The expansion and migration rate of the monolayer exhibited a strong negative correlation. The study highlights the importance of initial boundary conditions in the collective cell migration of the expanding tissue and provides useful insights that might be helpful in the future to tune the collective cell migration in wound healing, cancer metastasis, and tissue formation.

11.
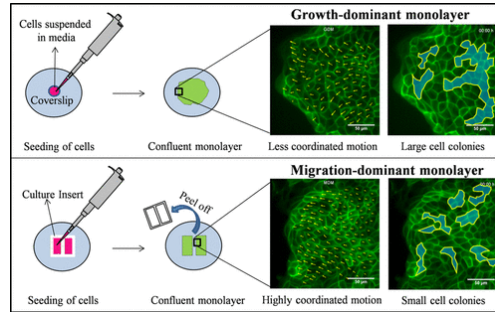
Droplet collision and jet evolution hydrodynamics in wetting modulated valley configurations
S Agrawal, G Khurana, P Dhar - Physics of Fluids, 2021

Abstract: Droplet impact hydrodynamics on "V"-shaped valleys or grooves of variant wettability and geometric dimensions have been studied experimentally and probed theoretically. The groove geometry makes the hydrodynamics three-dimensional, as in addition to the droplet dynamics in the lateral direction, liquid jets are generated from the post-impact droplet along the axial direction of the groove. The effect of the impact Weber number (We) on the jet velocity, the non-dimensional spreading width (γ), and north-pole height (h*) has been studied. It has been observed that the inertial forces dominate over the surface forces for higher impact We and hence, the effect of wettability is not important. However, the wettability of the substrate has a significant role in lower impact We as recoiling of the droplet is observed for the impact on the superhydrophobic substrate in this case. It has been observed that the spreading width of the post-impact droplet decreases with the increase in groove steepness. The jetting hydrodynamics has been probed and instantaneously after the impact, the generated jets travel at high velocity, but quickly reduce to a steady value. Jet velocity is observed to increase with an increase in the hydrophobicity of the substrate as well as the impact We. A semi-analytical formalism has been proposed to predict the jet velocity evolution in terms of governing Weber (We) and capillary (Ca) numbers. The predictions from the proposed model are in good agreement with the experimental results.

12.

Effect of Salinity on Moisture Flow and Root Water Uptake in Sandy Loam Soil
S Kumar, I Sonkar, V Gupta, KS Hari Prasad, CSP Ojha - Journal of Hazardous, Toxic , and Radioactive Waste, 2021

Abstract: The present study analyzes the effect of salinity on crop growth and root zone soil moisture dynamics. A newly developed root water uptake (RWU) model was used for simulation of soil moisture and RWU for irrigation field experiments where paddy was grown with irrigation water with varying salinity concentrations (0.5, 7.9, 14.7, and 21.2 dS/m). The growth of the crop was monitored regularly, and crop parameters such as leaf area index (LAI) and root depth along with the soil moisture profile were measured during the crop growth period. The nonlinear parameter for the RWU model was estimated using an empirical relation in terms of

observed crop variables (LAI and root depth) for each saline irrigation condition. Root zone soil moisture and RWU for the prevailing hydrometeorological conditions during the crop period and soil-crop parameters were simulated for the analysis. The irrigation experiments show that the growth of the crop is significantly affected by the salt concentration in soil-water, resulting in a decrease in the crop canopy (LAI) and root depth decreases with an increase in the salt concentration. The model simulation results show that an increase in salt concentration in irrigation water results in reduced root water extraction and reduced moisture content in the soil profile.

13.

Effect of Sinusoidally Varying Flow of Yield Stress Fluid On Heat Transfer From a Cylinder
S Gupta, S Patel, RP Chhabra - Journal of Heat Transfer, 2021

Abstract: The effect of pulsating laminar flow of a Bingham plastic fluid on heat transfer from a constant temperature cylinder is studied numerically over wide ranges of conditions as Reynolds number ($0.1 \leq Re \leq 40$) and Bingham number ($0.01 \leq Bn \leq 50$) based on the mean velocity, Prandtl number ($10 \leq Pr \leq 100$), pulsation frequency ($0 \leq \omega^* \leq \pi$), and amplitude ($0 \leq A \leq 0.8$). Results are visualized in terms of instantaneous streamlines, isotherms, and apparent yield surfaces at different instants of time during a pulsation cycle. The overall behavior is discussed in terms of the instantaneous and time-averaged values of the drag coefficient and Nusselt number. The size of the yielded zone is nearly in phase with the pulsating velocity, whereas the phase shift has been observed in both drag coefficient and Nusselt number. The maximum augmentation (~30%) in Nusselt number occurs at $Bn = 1$, $Re = 40$, $Pr = 100$, $\omega^* = \pi$, and $A = 0.8$ with respect to that for uniform flow. However, the increasing yield stress tends to suppress the potential for heat transfer enhancement. Conversely, this technique of process intensification is best suited for Newtonian fluids in the limit of $Bn \rightarrow 0$. Finally, a simple expression consolidates the numerical values of the time-averaged Nusselt number as a function of the pertinent dimensionless parameters, which is consistent with the widely accepted scaling of the Nusselt number with $\sim Pe^{1/3}$ under these conditions.

14.

Elastic instabilities and bifurcations in flows of wormlike micellar solutions past single and two vertically aligned microcylinders: Effect of blockage and gap ratios
MB Khan, C Sasmal - Physics of Fluids, 2021

Abstract: This study presents an extensive numerical investigation on the flow characteristics of wormlike micellar (WLM) solutions past a single and vertically aligned two microcylinders placed in a microchannel in the creeping flow regime. The rheological behavior of the micellar solution is realized based on the two-species Vasquez–Cook–McKinley (VCM) constitutive model, which takes into account both the breakage and re-formation dynamics of micelles. For the case of single microcylinder, as the blockage ratio (ratio of the cylinder diameter to that of the channel height) is gradually varied, we find the existence of a flow bifurcation in the system, and also a gradual transition for a range of flow states, for instance, steady and symmetric or Newtonian like, steady and asymmetric, unsteady periodic and asymmetric, unsteady quasi-periodic and asymmetric, and, finally, unsteady quasi-periodic and symmetric. For the case of two microcylinders, we observe the presence of three distinct flow states in the system, namely diverging (D), asymmetric-diverging (AD), and converging (C) states as the intercylinder spacing in between the two cylinders is varied. Similar types of flow states are also observed in the recent experiments dealing with WLM solutions. However, we show that either this transition from one flow state to another in the case of a single microcylinder or the occurrence

	of any flow state in the case of two microcylinders is strongly dependent upon the values of the Weissenberg number and the nonlinear VCM model parameter ξ, which basically indicates how easy or hard it is to break a micelle. Based on the results and discussion presented herein for the single and two microcylinders, we hope this study will facilitate the understanding behind the formation of preferential paths or lanes during the flow of viscoelastic fluids through a porous media, which was seen in many prior experiments in the creeping flow regime.
15.	EWS: Exponential Windowing Scheme to Improve LoRa Scalability D Saluja, R Singh, S Gautam, S Kumar - IEEE Transactions on Industrial Informatics, 2021 **Abstract:** Internet-of-Things (IoT) applications require a network that covers a large geographic area, consumes less power, is low-cost, and is scalable with an increasing number of connected devices. Low-power wide-area networks (LPWAN) have recently received significant attention to meet these requirements of IoT applications. LoRaWAN with LoRa (the physical layer design for LoRaWAN) has emerged as a leading LPWAN solution for IoT.}} However, LoRa networks suffer from the scalability issue when supporting a large number of end devices (EDs) that access the shared channels randomly. The scalability of LoRa networks greatly depends on the spreading factor (SF) allocation schemes. In this work, we propose an exponential windowing scheme (EWS) for LoRa networks to improve the scalability of LoRa networks. EWS is a distance-based SF allocation scheme. It assigns a distance parameter to each spreading factor (SF) to maximize the success probability of the overall LoRa network. Using stochastic geometry, expressions for success probability are derived under co-SF interference. The impact of exponential windowing and packet size is analyzed on packet success probability. In addition, the proposed scheme is compared with the existing distance-based SF allocation schemes: equal interval-based (EIB) and equal area-based (EAB) schemes, and it is shown that the proposed scheme performs better than the other two schemes.
16.	Experimental study of a combined biomass and solar energy-based fully grid-independent air-conditioning system G Singh, R Das - Clean Technologies and Environmental Policy, 2021 **Abstract:** In this paper, a small-scale triple-hybrid air-conditioning system operated by biomass and solar energy resources is experimentally investigated. Comparisons with EnergyPlus simulations are also shown. Experiments reveal the necessity of system's pull down because of inequality of heat transfer within the chiller. The biomass gasifier driving an electrical generator in combination with solar collector fulfils the total energy requirements that make the present system triple-hybrid in nature. An air-cooled lithium bromide–water operated absorption chiller of 4.06 kW rated capacity is fabricated and tested. The biomass-generated electricity enables to reduce the grid dependency of the system to fulfil net-zero-energy criterion. The system is tested under different generator temperature ranges (60 °C, 70 °C and 80 °C) and lithium bromide concentrations (54% and 58%) in water. With 54% concentration, this system operates up to 64.8% of nominal capacity with average coefficient of performance ranging between 0.14 and 0.19. However, with 58% concentration, up to 85.1% of its nominal capacity along with the coefficient of performance ranging between 0.19 and 0.25 can be acquired. The system caters the maximum load with the highest coefficient of performance of 0.34. Rise in the generator temperature improves the cooling capacity, coefficient of performance, shows quicker response of the system and drops the finally-attained room air temperature. Economic analysis reveals the payback time for the present system to lie in the range of 9–12 years. Finally, emission analysis

reveals considerable possibility of greenhouse gas reduction in an affordable manner.

Graphical Abstract:
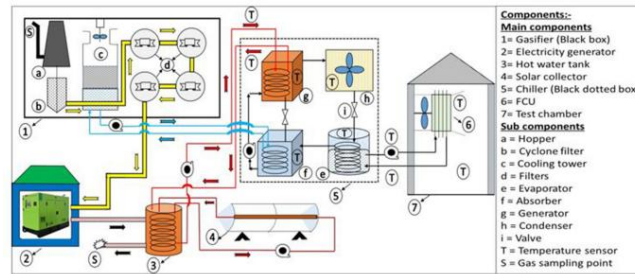
[Experimental Study on a New Small-Scale Absorption System: Response Surface and Inverse Analyses](#)
G Singh, R Das - Journal of Energy Resources Technology, 2021

Abstract: In this paper, a new small-scale lithium bromide (LiBr)-water absorption system consisting water-cooled evaporator and air-cooled condenser is experimentally studied. For compactness, water-cooled heat exchangers for evaporator, absorber and generator are made helical-coiled type, whereas, based on the water availability and load requirements, condenser is air-cooled. Accurate empirical correlations for thermal load and evaporator temperature against system driving factors concerning a have been reported. Thereafter, response surface analysis of the developed performance parameters are studied with respect to LiBr concentration, temperature of generator and mass flow rate of hot water. Using experimental data, estimation of overall heat transfer coefficient (U) and its variation with system driving factors is quantified. The error margin between theoretical and actual pressure loss is limited within 5 %. Next, a multi-objective inverse analysis of the developed system is done to simultaneously retrieve the required LiBr concentration, mass flow rate of hot water, and vapor generator temperature to derive a desired cooling performance demand from the system. The obtained U values for all the components are found to be in line with the standard data. The physics related to salt concentration and generator temperature in governing U values are reported. Apart from the developed correlations, it can be established that the necessary operational parameters can be predicted by the present multi-objective inverse method to meet the necessary thermal load and temperature demands within an accuracy level of 6 % and 5 %, respectively.

[FakeBuster: A DeepFakes Detection Tool for Video Conferencing Scenarios](#)
V Mehta, P Gupta, R Subramanian, A Dhall - 26th International Conference on Intelligent User Interfaces, 2021

Abstract: This paper proposes FakeBuster, a novel DeepFake detector for (a) detecting impostors during video conferencing, and (b) manipulated faces on social media. FakeBuster is a

standalone deep learning- based solution, which enables a user to detect if another person's video is manipulated or spoofed during a video conference-based meeting. This tool is independent of video conferencing solutions and has been tested with Zoom and Skype applications. It employs a 3D convolutional neural network for predicting video fakeness. The network is trained on a combination of datasets such as Deeperforensics, DFDC, VoxCeleb, and deepfake videos created using locally captured images (specific to video conferencing scenarios). Diversity in the training data makes FakeBuster robust to multiple environments and facial manipulations, thereby making it generalizable and ecologically valid.

19.	[Fine-finishing of stepped cylindrical workpiece using magnetorheological finishing process](#) AS Rana, TS Bedi, V Grover - Materials Today: Proceedings, 2021 **Abstract:** A various stepped cylindrical workpieces are commonly known for their functionality in different industrial components such as hydraulic or pneumatic actuators, plungers, etc. However, fine-finishing of stepped cylindrical workpiece (made of softer materials) is difficult by grinding operation because of its rigid tool structure. This tool structure is made by the rigid bonding of abrasive particles to a comman wheel. When this rigid tool approaches the workpiece surface, it results with different surface defects such as pits, scratches, grooves, cavity, etc. To overcome such circumstances, magnetorheological (MR) processes can be used. These processes use MR polishing fluid for fine-finishing of different materials ranging from soft to the harder type. In the present work, the MR finishing process is used for finishing of the external surfaces of stepped cylindrical workpiece. The MR finishing tool is developed in such a way that it is flexible in accordance with the diameter of cylindrical workpiece. In this tool structure, the permanent magnets (made up of neodymium NdFe35) have been used for retaining the MR polishing fluid on its surface. Experiments have been conducted on the aluminium stepped workpiece in order to check the practicability of the present developed tool. The results revealed that a fine-finishing of stepped cylindrical workpiece with a surface roughness Ra value as 62 nm is achieved on aluminium workpiece. Also, the mechanism of material removal involved during the finishing process has been analyzed mathematically. Removal of material from the external surface of single step of aluminium workpiece has been confirmed mathematically with the help of the present developed MR finishing tool.
20.	[First-principles study of 2-dimensional C-silicyne monolayer for promising anode in Na/K ion secondary battery](#) N Yadav, B Chakraborty, DTJ Kumar - Physical Chemistry Chemical Physics, 2021 **Abstract:** With the depleting resources of energy and increasing demand over the top, the need for sustainable and renewable energy resources has become the need of an hour. The low storage capacity of present materials for Na/K ion battery invites the quest to identify suitable materials for an electrode having excellent electrochemical properties. In the presented work, systematic theoretical investigation of C-silicyne, a planar 2-dimensional hexagonal lattice, is performed to establish geometric, thermal and stability. The electronic properties illustrate the metallic nature of C-silicyne which is conserved even after effective adsorption of Na/K ion on the surface of the monolayer. For practical functionality, the storage capacity of C-silicyne is evaluated as 591 mAh/g for Na ion and 443 mAh/g for K ion. Moreover, a low diffusion barrier for Na (0.57 eV) and K (0.34 eV) ions display their feasible movement across the monolayer as the electrochemical cycle progresses. The average working voltage is found to lie in the range (0.1-1 V) for the effective functioning of the anode in Na/K ion battery. These results bring up the

potential of C-silicyne as a material for anode electrode in Na/K ion battery application.

21.	**Flow of Power-Law Fluids Past a Rotating Cylinder At High Reynolds Numbers** P Thakur, N Tiwari, RP Chhabra - Journal of Fluids Engineering **Abstract:** In this study, a rotating cylinder is placed in a stream of shear-thinning fluids, flowing with an uniform velocity. Detailed investigations are performed for the following range of conditions: Reynolds number $100 \leq Re \leq 500$, power-law index $0.2 \leq n \leq 1$ and rotational velocity $0 \leq \alpha \leq 5$. Flow transitions are observed from steady to unsteady at critical values of the Reynolds number, the rotational velocity, and the power-law index. Critical values of the Reynolds number Re_c have been obtained for varying levels of the rotational velocity, and the power-law index. Re_c varies non-monotonically with the rotational velocity. At a particular Reynolds number, an increase of the rotational velocity acts as a vortex suppression technique. For shear-thinning fluids considered here, the vortex suppression occurs at a larger value of the critical rotational velocity α_c, relative to Newtonian fluids. For the unsteady flow, lift coefficient versus time curve exhibits oscillatory behaviour, and this has been used to delineate the flow regime as steady or unsteady flow. For unsteady flow regimes, both the amplitude of the lift coefficient and the Strouhal number increase with increasing Reynolds numbers. The results presented in this work for such high Reynolds numbers elucidate the possible complex interplay between the kinematic and rheological parameters of non-Newtonian fluids. This investigation also complements the currently available low Reynolds number results up to $\sim Re = 140$.
22.	**Frequency Modulated Thermal Wave Imaging for Infrared Non-destructive Testing of Mild Steel** A Rani, R Mulaveesala - MAPAN, 2021 **Abstract:** Frequency modulated thermal wave imaging (FMTWI) has been successfully applied in the field of infrared thermography to estimate defects in various structural materials. The paper presents theoretical aspects of three-dimensional mild steel sample for FMTWI to detect flat bottom holes as defects. Furthermore, performance of FMTWI for analytical and simulated approach has been discussed and comparison has been performed based on time domain matched filtering pulse compression approach. The results demonstrate enhanced depth resolvability of the time domain-based pulse compression approach for FMTWI scheme.
23.	**Influence of injection and holding pressure on tribological and mechanical behavior of injection moulded thermoplastic** R Yadav, A Pancharya, R Kant - Materials Today: Proceedings, 2021 **Abstract:** Injection moulding is used significantly in modern days for manufacturing of plastic materials, mainly due to its effectiveness of mass production, modulation of complex geometry, and high precision objects. The process is influenced by various parameters like mould temperature, injection pressure, holding pressure, cooling arrangement, cooling time, injection speed and melt temperature, resulting in effective manufacturing with a quality product. The current study is focused on analysing the influence of injection pressure and holding pressure on the fabrication of Delrin specimens. Delrin is one of the most commonly used plastic for wear-related issues, mainly due to its higher wear resistance and sliding properties. In this study, the effect of injection pressure and holding pressure is analysed on the mechanical and tribological properties of Delrin specimen, for which pin on disc and universal testing machine are used, respectively. Experimental results showed that the wear resistance, tensile strength and compressive strength of Delrin specimens were increased with respect to the injection pressure

|	
	up to a specific limit but continuously increased with the holding pressure.
24.	Influence of Thickness of Hydrophobic Polytetrafluoroethylene (PTFE) Coatings on Cavitation Erosion of Hydro-machinery Steel SS410 A Bansal, J Singh, H Singh, DK Goyal - Wear, 2021 **Abstract:** Hydrophobic materials have the potential to replace the existing surface modification materials to combat the problem of cavitation erosion (CE), owing to their various capabilities like self-cleaning, anti-corrosion, anti-fogging, anti-icing, anti-fouling, and drag-reduction. Polytetrafluoroethylene (PTFE) as a hydrophobic material exhibits specific combination of properties such as low friction coefficient, chemically neutral, good impact strength and considerable thermal firmness, that allow PTFE to be used in a wide range of applications. Therefore, in this work, an effort has been made to explore the effect of thickness of hydrophobic PTFE coatings on CE of the hydro-machinery SS410 steel. Hydrophobic PTFE coatings with three variable thicknesses have been prepared on the hydro-machinery SS410 steel using sintering process. Using high-velocity submerged water jet cavitation erosion test rig, CE behaviour of PTFE coated and bare SS410 steel was evaluated under various combinations of operating parameters: namely jet velocity, stand-off distance (SOD), and impact angle. Contact angle was reported to be increased with the decrease in the thickness of PTFE layer, which may be due to the increased surface roughness of PTFE layer with decrease in thickness. CE resistance of PTFE coated material with a maximum thickness of 121 μm, was found to be highest for all the combinations of operating parameters, which may be attributed to its lowest fracture toughness and better cushioning effect. Further, it was observed that CE of the coated and SS410 steel was found to be maximum at the chosen maximum velocity, normal impact angle, and intermediate SOD. The signatures of pits with circular and elongated morphology were observed for normal and shallow impact angles, respectively. In case of lowest PTFE layer thickness, overlapped pits with relatively higher depth were observed, which might be responsible for higher CE of the same amongst all the PTFE coatings.
25.	InfraRed image correlation for non-destructive testing and evaluation A Rani, V Arora, R Mulaveesala - Proceedings Volume 11743, Thermosense: Thermal Infrared Applications XLIII, 2021 **Abstract:** InfraRed Thermography (IRT) is one of the widely used Non-destructive Testing and Evaluation (NDT and E) method for characterization of fiber reinforced polymers. Among various testing methodologies and associated post processing schemes, recently proposed pulse compression favorable thermal wave imaging methodologies gained importance due to their enhanced test sensitivity and resolution for identifying the sub-surface defects. The present paper highlights a highly depth resolved pulse compression favorable thermal wave imaging methodology for identification of subsurface defects in a Glass Fiber Reinforced Polymer (GFRP) test specimen.
26.	Inverse Power Law based Inclusive Life Model for DC Polarity Reversal Stresses C Lyyappan, CC Reddy - IEEE Transactions on Dielectrics and Electrical Insulation, 2021 **Abstract:** In this paper, carefully designed experiments are reported, which indicate that the change in frequency of voltage polarity reversals results in a change in slope of v-t characteristics on the inverse power law. The power law parameters are shown to be systematic functions of frequency of polarity reversals. Based on these results, the authors propose a

comprehensive inverse power law for DC polarity reversal stress application, in place of conventional inverse power law. The proposed modification is examined with experimental data of authors apart from that available in literature and found to be working well. The model provides the maximum frequency of a reversal for maximizing the life of power equipment which may pave the way for deciding on the maximum frequency of voltage reversals.

27.

Investigating slurry erosion behavior of a hydro-machinery steel under various impingement variables
A Bansal, J Singh, H Singh - Materials Today: Proceedings, 2021

Abstract: SS410 is widely used as a hydro-machinery steel and is generally exposed to the slurry erosion conditions, which decrease its useable-life. In the current investigation, an attempt was made to analyse the effect of slurry erosion on this steel. The slurry erosion testing was done in a slurry erosion test rig, which provides possibility to vary impingement conditions like average particle size, slurry concentration, impingement angle, and velocity of jet. Moreover, some mechanical and metallurgical properties of the steel were also investigated. It was concluded that the slurry erosion rate of the steel increases with increase in the concentration and jet velocity. However, with the increase in average particle size, slurry erosion was found to decrease, which may be due to the lower penetration capacity of higher sand particles. Moreover, slurry erosion, in general, was found to be maximum at a parametric combination of lowest average particle size (150 µm), 60° impingement angle, maximum concentration (45000 ppm), and maximum jet velocity (35 m/sec). Slurry erosion was found to be maximum at an impingement angle of 60°, indicating a mixed mode of erosion (ductile as well as brittle) for the given steel. The mechanisms involved in slurry erosion were found to be crater formation, ploughing, and lip formation followed by its fracture.

28.

Investigation of Limitations in Active Damping Control of LCL Filter Resonance using Inverter Side Current Feedback in Grid Connected Voltage Source Converter
S Muddasani, AVR Teja - IEEE Texas Power and Energy Conference, 2021

Abstract: This paper investigates the active damping of LCL filter resonance in a grid connected voltage source inverter. The active damping realized using feedback of inverter side current is considered for analysis. A detailed study showing suitable choice of resistor required for resonance damping in case of the passive and active damping methods is presented. An explicit study showing the limitations of active damping over passive damping for a chosen Switching and resonance frequencies has carried out. The proposed work is simulated using MATLAB/Simulink for the resonance frequency of 1.4kHz and switching frequency of 10KHz. Typical results are reported and analyzed. It is observed from results that the virtual resistor introduced using active damping technique is unlike to the passive damping after a point of Rd values. This issue can be resolved by choosing controller bandwidth adaptive to the changes present in value of virtual resistor.

29.

Phase stability and microstructural evolution of Ti2AlNb alloys-a review
K Goyal, N Sardana - Materials Today: Proceedings, 2021

Abstract: Ti2AlNb alloys are potential next-generation aerospace materials due to their lightweight and high-temperature strength and oxidation resistance properties. Heat treatment of this alloy results in five major microstructures, including fully B2 and $\alpha2 + B2$, lamellar, bimodal lamellar, equiaxed, and duplex O-phase microstructure. Recently, widmanstätten and plate-like

|	
	O phase have also been reported. Modern manufacturing methods have made fabrication of high-temperature alloys easy and economical. However, they need post-heat treatments to improve the microstructure and mechanical properties. In this review article, a sequence of various developments in the study of features and thermo-mechanical control on the evolution of various microstructures of the Ti2AlNb intermetallic alloys will be presented. In addition, other aspects such as orientation relationships between different phases, factors affecting grain growth and, phase evolution mechanisms will be discussed. The effect of each heat treatment on every feature of the microstructure will be summarized in each section.
30.	Pole skipping and chaos in anisotropic plasma: a holographic study K Sil - Journal of High Energy Physics, 2021 **Abstract:** Recently, a direct signature of chaos in many body system has been realized from the energy density retarded Green's function using the phenomenon of 'pole skipping'. Moreover, special locations in the complex frequency and momentum plane are found, known as the pole skipping points such that the retarded Green's function can not be defined uniquely there. In this paper, we compute the correction/shift to the pole skipping points due to a spatial anisotropy in a holographic system by performing near horizon analysis of EOMs involving different bulk field perturbations, namely the scalar, the axion and the metric field. For vector and scalar modes of metric perturbations we construct the gauge invariant variable in order to obtain the master equation. Two separate cases for every bulk field EOMs is considered with the fluctuation propagating parallel and perpendicular to the direction of anisotropy. We compute the dispersion relation for momentum diffusion along the transverse direction in the shear channel and show that it passes through the first three successive pole skipping points. The pole skipping phenomenon in the sound channel is found to occur in the upper half plane such that the parameters Lyapunov exponent λ_L and the butterfly velocity v_B are explicitly obtained thus establishing the connection with many body chaos.
31.	Predicting women with depressive symptoms postpartum with machine learning methods S Andersson, DR Bathula, SI Iliadis, M Walter, A Skalkidou - Scientific Reports, 2021 **Abstract:** Postpartum depression (PPD) is a detrimental health condition that affects 12% of new mothers. Despite negative effects on mothers' and children's health, many women do not receive adequate care. Preventive interventions are cost-efficient among high-risk women, but our ability to identify these is poor. We leveraged the power of clinical, demographic, and psychometric data to assess if machine learning methods can make accurate predictions of postpartum depression. Data were obtained from a population-based prospective cohort study in Uppsala, Sweden, collected between 2009 and 2018 (BASIC study, $n = 4313$). Sub-analyses among women without previous depression were performed. The extremely randomized trees method provided robust performance with highest accuracy and well-balanced sensitivity and specificity (accuracy 73%, sensitivity 72%, specificity 75%, positive predictive value 33%, negative predictive value 94%, area under the curve 81%). Among women without earlier mental health issues, the accuracy was 64%. The variables setting women at most risk for PPD were depression and anxiety during pregnancy, as well as variables related to resilience and personality. Future clinical models that could be implemented directly after delivery might consider including these variables in order to identify women at high risk for postpartum depression to facilitate individualized follow-up and cost-effectiveness.

32.	[Prediction of Heat-Generation and Electromagnetic Parameters from Temperature Response in Porous Fins](#) R Das, B Kundu - Journal of Thermophysics and Heat Transfer, 2021 **Abstract:** The application of combined electric and magnetic fields is proposed for better heat transfer enhancement in a porous fin system. An inverse estimation technique is established to simultaneously determine the interior thermal energy production and strengths of electrical and magnetic fields, by solely using the surface temperature field. At first, verified direct solutions based on the fourth-order Runge–Kutta method are obtained for the computation of the temperature field, and then three unidentified parameters are estimated using the inverse procedure supported by the Artificial Bee Colony (ABC) algorithm. The corresponding analytical solution is evaluated using the differential transformation method. The existing investigation demonstrates that even though various parametric groups sustain a particular thermal field, amongst them, the nearly unique value of the thermomagnetic field governs the heat transport phenomena. Additionally, the joint interaction between the electric field and thermal-energy-generation parameter is accountable for the observed temperature field. In spite of the effect of random noise levels within $+/- 11\%$, the ABC-based inverse solution technique is found to establish the thermal criteria and to excellently reconstruct the given thermal field within a less than 1% error margin with respect to the ideal situation. For any case, 50 iterations of ABC are observed to be satisfactory. For fulfilling the desired rate of thermal energy transfer from porous fins, the present prediction scheme is suggested to be beneficial in properly adjusting the electrical and magnetic fields along with the unknown state of thermal energy production.
33.	[Pressure-Driven Membrane Process: A Review of Advanced Technique for Heavy Metals Remediation](#) B Verma, C Balomajumder, M Sabapathy, SP Gumfekar - Processes, 2021 **Abstract:** Pressure-driven processes have come a long way since they were introduced. These processes, namely Ultra-Filtration (UF), Nano-Filtration (NF), and Reverse-Osmosis (RO), aim to enhance the efficiency of wastewater treatment, thereby aiming at a cleaner production. Membranes may be polymeric, ceramic, metallic, or organo-mineral, and the filtration techniques differ in pore size from dense to porous membrane. The applied pressure varies according to the method used. These are being utilized in many exciting applications in, for example, the food industry, the pharmaceutical industry, and wastewater treatment. This paper attempts to comprehensively review the principle behind the different pressure-driven membrane technologies and their use in the removal of heavy metals from wastewater. The transport mechanism has been elaborated, which helps in the predictive modeling of the membrane system. Fouling of the membrane is perhaps the only barrier to the emergence of membrane technology and its full acceptance. However, with the use of innovative techniques of fabrication, this can be overcome. This review is concluded with perspective recommendations that can be incorporated by researchers worldwide as a new problem statement for their work.
34.	[R-Comm: A Traffic Based Approach for Joint Vehicular Radar-Communication](#) R Singh, D Saluja, S Kumar - IEEE Transactions on Intelligent Vehicles, 2021 **Abstract:** Automotive radar and vehicular communication are the two primary means of establishing an intelligent transportation system. However, both the systems are susceptible to

interference. The inter-vehicular interference significantly affects the radar and communication performance, especially in the dense traffic scenarios. In this work, we have shown that lowering down radar range in dense traffic scenario provides twofold advantages; (a) it reduces radar-to-radar interference and, (b) it provides resources to support the vehicular communication. We propose a joint Radar-Communication (R-Comm) algorithm which enables connected vehicles to use a fraction of radar resources for vehicular communication based on the traffic density. Also, two different schemes have been proposed for R-Comm transmission in the sparse and dense traffic scenarios. Further, through simulation results, it is shown that R-Comm benefits both the radar and communication systems.

35.

[Reductive Formylation of Nitroarenes using HCOOH over Bimetallic C-N Framework Derived from the Integration of MOF and COF](#)
R Srivastava, AK Kar – ChemCatChem, 2021

Abstract: CoZn embedded C-N framework is prepared by the carbonization of CoZn containing MOF integrated with COF porous architecture in Ar atmosphere. The graphitic nature of porous carbon is confirmed from Raman analysis. The porosity and nanostructure information are retrieved from N2-sorption and transmission electron microscopic analysis, respectively. The incorporation of different metals & their oxidation states and types of nitrogen present in the C-N framework are confirmed from X-ray photoelectron spectroscopy. The basicity of the materials is determined from a CO2-temperature programmed desorption. ZnCo embedded C-N framework exhibits excellent activity in the selective reductive formylation using HCOOH. For comparison, more than 15 materials are prepared, and their activities are compared. Several control experiments are performed to establish a structure-activity relation. The recycling experiment, hot-filtration test, and poisoning experiment demonstrate the metal embedded porous C-N framework's recyclability and stability. A reaction mechanism for the reductive N-formylation of nitroaromatics is presented based on structure-activity relationship, control reactions, and physicochemical characterizations. The development of interesting MOF-COF-derived metal nanoclusters embedded C-N framework for selective reductive formylation of nitroaromatics using formic acid will be highly attractive to catalysis researchers and industrialists.

36.

[Relieving the Stress Together: Annulation of Two Different Strained Rings Towards the Formation of Biologically Significant Heterocyclic Scaffolds](#)
A Ghosh, R Dey, P Banerjee - Chemical Communications, 2021

Abstract: Owing to their intrinsic ring strain and ease of synthesis, small carbo- and heterocycles became versatile building blocks. However, the traditional approaches of heterocycle synthesis involved the combination of one strained-carbocycle or heterocycle with one unsaturated molecule. On the contrary, there is an exciting possibility of combining two different strained rings to furnish varieties of heterocycles where one of the strained rings can act as a valuable alternative to the unsaturated molecule. These strategies are also useful to access multi-functionalized rings. Despite these distinctive synthetic benefits, this chemistry has not gained a considerable attraction to the community. In this minireview, we explicitly choose this topic to reveal the unexplored possibilities with these different strained rings. This minireview will give a comprehensive detail with mechanistic rationale about the reactivity of these pairs of small rings when they are allowed to react together in the presence of different Lewis acids. Subsequently, it will also open a new avenue for heterocycle synthesis.

37.	[Solar Interfaced Series Inverter with Provision of Common DC bus Grounding](#) BK Gupta, SR Kondapalli, AI Gedam - IEEE Transactions on Industrial Electronics, 2021 **Abstract:** In this work, a new series modular solar inverter configuration is proposed to share the power in terms of voltage, unlike parallel inverter configurations. In a single-stage parallel inverter, elevated DC potential and circulating current due to common-mode voltage (CMV) would degrade the solar inverter's life. The proposed topology eases the stress on the DC bus and protects the solar inverter from the issues associated with elevated DC potential (Potential induced degradation effect, switch operating voltage stress, etc.). The inherent boosting capability of the proposed series inverter with two two-level inverters is demonstrated through two switching algorithms. In the first switching algorithm, the switching combinations are devised to yield the maximum voltage across the load. The second switching algorithm demonstrates the method of eliminating CMV by choosing the appropriate switching combination of two inverters. The eliminated instantaneous CMV would give the provision of operating proposed topology with common DC bus along with the flexibility of DC bus grounding. For the proposed configuration with devised switching techniques, the closed-loop controller is designed by computing the plant's equivalent characteristic impedance using a state-space model. The effectiveness of the proposed configuration, along with the closed-loop control, is validated through hardware.
38.	[Squaramide Catalyzed Asymmetric Synthesis of Five-and Six-Membered Rings](#) I Chatterjee, A Biswas, A Ghosh, R Shankhdhar - Asian Journal of Organic Chemistry, 2021 **Abstract:** Chiral analogues of squaramides have been fruitful in organocatalyzed asymmetric reactions over last decade. Alongside other H-bonding catalysts like ureas, thioureas: squaramides have been proved to be efficient asymmetric catalysts for the formation of acyclic and cyclic chiral molecules. A wide range of cyclic molecules bearing multiple functionalities and stereocenters have been synthesized by using several bifunctional squaramides as catalysts. These catalysts perform as base utilizing basic N atom in their chiral extension and help in stereoinduction by forming H-bonds with suitable H-bond acceptors. The present review focuses on assembling recent progresses of asymmetric synthesis of five and six membered rings promoted by squaramides. A handful of articles have been published by several research groups documenting asymmetric construction of five- and six-membered rings as part of interesting and complex molecular architectures. Different methodologies like conventional and formal cycloadditions or cascade reactions have been engineered through the assistance of chiral squaramides to fabricate the carbo- and heterocycles. This review also includes dual and cooperative catalytic system in which squaramide is one of the catalysts.
39.	[Superflexible, Self-Biased, High-Voltage-Stable, and Seal-Packed Office-Paper Based Gallium-Oxide Photodetector](#) K Arora, K Kaur, M Kumar - ACS Applied Electronic Materials, 2021 **Abstract:** This research presents a solar-blind (UVC) office paper-based photodetector that is self-biased, superflexible, nonwettable, high-performance, and high-voltage stable. In contrast to the traditional design of photodetectors involving sophisticated techniques, this study reports unique and facile hand-sketched bottom asymmetric graphite and silver electrodes. The asymmetric bottom electrodes offer minimum reflectivity that limits the dark current to 1.2 pA and boosts the device performance even at zero bias; this results in a significantly increased

On/Off ratio of more than 104 at 254 nm. The photodetector exhibits high responsivity (3.1 mA W–1), and fast response (0.459 s/0.386 s), even at zero bias. For good formability deformations (30 cm–1) as well as for wide turning angles (±180°), a high strenuous durability test demonstrated impressive photoswitching characteristics. Highly stable bottom electrodes contributed to the exceptionally stable operation (>720 h) and much enhanced performance along with tremendous capability of bearing high voltages up to 100 V. The performance of the reported photodetector has considerably exceeded previously published photodetectors even on costly nonflexible substrates. Moreover, the paper-based device was coated with UV transparent enamel paint to make it completely protected from wettability.
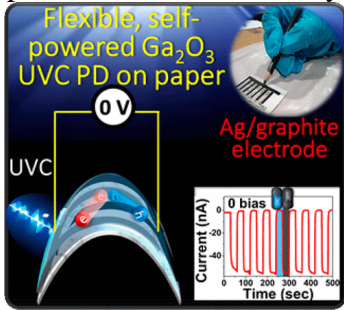
40.

[Synchrotron x-ray diffraction studies of the α⇌ β structural phase transition in Sn and Sn-Cu](#)
A Mazumdar, A Thamizhavel, V Nanal, RG Pillay… - Scripta Materialia, 2021

Abstract: The transformation between the metallic (β) and semiconducting (α) allotropes of tin is still not well understood. The phase transition temperature stated in the literature, 286.2 K, seems to be inconsistent with recent calorimetric measurements. In this paper, this intriguing aspect has been explored in Sn and Sn-Cu (alloyed 0.5% Cu by weight) using temperature resolved synchrotron x-ray diffraction measurements performed at the Indus-2 facility. Additionally, the α⇌β Sn transition has been recorded using in-situ heating/cooling experiments in a scanning electron microscope. Based on these measurements, a protocol has been suggested to reduce the formation of α-Sn in potentially susceptible systems. This will be useful in experiments like *TIN.TIN* (The INdia-based TIN detector), which proposes to employ ~100 - 1000 kg of superconducting tin-based detectors to search for neutrinoless double beta decay in the isotope [124]Sn.

Graphical Abstract:
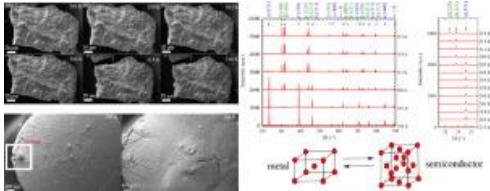
41.

[Unstable miscible displacements in radial flow with chemical reactions](#)
MC Kim, S Pramanik, V Sharma, M Mishra - Journal of Fluid Mechanics, 2021

Abstract: The effects of the A+B→C chemical reaction on miscible viscous fingering in a radial source flow are analysed using linear stability theory and numerical simulations. This flow and transport problem is described by a system of nonlinear partial differential equations consisting

of Darcy's law for an incompressible fluid coupled with nonlinear advection–diffusion–reaction equations. For an infinitely large Péclet number (Pe), the linear stability equations are solved using spectral analysis. Further, the numerical shooting method is used to solve the linearized equations for various values of Pe including the limit Pe→∞. In the linear analysis, we aim to capture various critical parameters for the instability using the concept of asymptotic instability, i.e. in the limit $\tau\to\infty$, where τ represents the dimensionless time. We restrict our analysis to the asymptotic limit Da∗ (=Daτ)→∞ and compare the results with the non-reactive case (Da=0) for which Da∗=0, where Da is the Damköhler number. In the latter case, the dynamics is controlled by the dimensionless parameter RPhys=$-(R_A-\beta R_B)$. In the former case, for a fixed value of RPhysRPhys, the dynamics is determined by the dimensionless parameter $R_{Chem}=-(RC-RB-RA)$. Here, β is the ratio of reactants' initial concentration and R_A, R_B and R_C are the log-viscosity ratios. We perform numerical simulations of the coupled nonlinear partial differential equations for large values of Da. The critical values $R_{Phys,c}$ and $R_{Chem,c}$ for instability decrease with PePe and they exhibit power laws in PePe. In the asymptotic limit of infinitely large Pe they exhibit a power-law dependence on Pe ($R_{Chem,c}\sim Pe^{-1/2}$ as Pe→∞) in both the linear and nonlinear regimes.
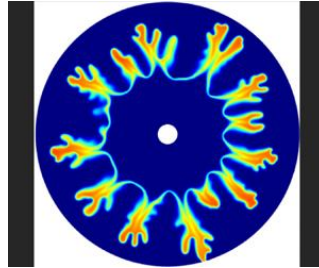
[Use of Cuckoo Search Algorithm for Performance Evaluation of Split Elliptic Shaped Fins for Enhanced Rate of Heat Transfer](#)
A Ranjan, R Das, S Pal, A Majumder, M Deb - Journal of Heat Transfer, 2021

Abstract: Proper dissipation of thermal energy has always been a need for desirable efficiency of a system. Extended surface aids in releasing the heat to the immediate surrounding by inducing an extra area. This particular work assesses thermal and fluid flow behavior of extended surfaces with circular and elliptic shaped cross section. Extended surfaces of unvaried cross section are mounted over a square plate arrayed in a staggered manner. With the aid of different thermofluidic parameters, the elliptic shaped pin fin is established to provide a higher thermal performance enhancement of nearly 15% over cylindrical pin fin at inlet flow velocity of 2.35 m/s. Further, for elevating the interaction between the surface of the fin and the fluid, elliptic fins are reoriented to form a split. In contrast to cylindrical shaped fin, modification using split shows better result with the highest heat transfer increment of nearly 25%. Further, in order to maximize Nusselt number (Nu), a single objective cuckoo search optimization analysis is done by adopting the response surface method. After analyzing the optimization, it is found that the maximum value of Nu is obtained at dimensionless transverse offset (TO*) = 0.125 and dimensionless longitudinal offset (LO*) = 0, which has been further validated with the numerical result within 0.97% accuracy. Further, for the cylindrical fin, the present simulations agree with the available empirical correlation within 6.22% accuracy.

43.	[User authentication using Blockchain based smart contract in role-based access control](#) P Kamboj, S Khare, S Pal - Peer-to-Peer Networking and Applications, 2021 **Abstract:** Since the last few decades, information security has become a significant challenge for organizations' system administrators. However, the Role-Based Access Control (RBAC) model has emerged as a viable solution for organizations to meet the security requirement due to its less administrative overhead. Blockchain technology is distributive and can be used effectively in user authentication and authorization challenges. This paper proposes an RBAC model using a blockchain-based smart contract for managing user-role permissions in the organization. We design a threat and security model to resist attacks such as man-in-the-middle attacks in an organization scenario. The proposed approach uses the Ethereum blockchain platform and its smart contract functionalities to model user-resource communications. The proposed method is tested on Ropsten Ethereum Test Network and evaluated to analyze user authentication, verification, cost, and security.
44.	[Vinylogous Aza-Michael Addition of Urea Derivatives with p-Quinone Methides Followed by Oxidative Dearomative Cyclization: Approach to Spiroimidazolidinone Derivatives](#) N Kaur, P Singh, P Banerjee - Advanced Synthesis & Catalysis, 2021 **Abstract:** Herein, we report an efficient protocol for the synthesis of spiro-imidazolidinone-cyclohexadienones from p-quinone methides (p-QMs) and dialkyloxy ureas under mild conditions. The strategy follows a two-step process involving an initial vinylogous conjugate addition of urea derivatives to p-QMs, followed by oxidative dearomative cyclization of open-chain product to the projected spiro-imidazolidinones. This protocol exhibits good functional group tolerance and provides a straightforward method to access spiro-imidazolidinone-cyclohexadienones. In follow-up chemistry, we have shown the debenzylation of spiroimidazolidinones to give N-hydroxycyclic ureas.
45.	[Viscous fingering of miscible annular ring](#) V Sharma, HB Othman, Y Nagatsu, M Mishra - Journal of Fluid Mechanics, 2021 **Abstract:** Miscible viscous fingering (VF) of the annulus of a more viscous fluid radially displaced by a less viscous fluid is investigated through both numerical computations and experimental study. We aim to understand how VF with finiteness in a radial displacement different from the classical radial VF and the instability of a slice displaced rectilinearly with a uniform velocity. It is observed that the VF of a miscible annular ring is a persistent phenomenon in contrast to the transient nature of VF of a miscible slice. Although new fingers cease to appear after some time but due to the radial spreading of the area available for VF, a finite number of fingers always remain at a later time when diffusion is the ultimate dominating force. A statistical analysis is performed for the numerical data and it is found that the second moment of the averaged profile, variance, is a non-monotonic function of time, contrary to variance in classical radial VF and rectilinear VF with one fluid sandwiched between layers of another. The minimum in the variance indicates the interaction of two fronts which is visible in terms of pressure fingers, but not the concentration fingers indicating a faster growth of pressure than the

concentration growth. In addition, for existence of critical parameters for instability in terms of viscosity contrast and amount of sample, the variation of the finger length with flow rate is found to be dependent on the amount of the more viscous fluid confined in the annulus.